Journal Pre-proofs

Discovery of a novel 2,3-dimethylimidazo[1,2-*a*]pyrazine-6-carboxamide M_4 positive allosteric modulator (PAM) chemotype

Kayla J. Temple, Julie L. Engers, Madeline F. Long, Katherine J. Watson, Sichen Chang, Vincent B. Luscombe, Matthew T. Jenkins, Alice L. Rodriguez, Colleen M. Niswender, Thomas M. Bridges, P. Jeffrey Conn, Darren W. Engers, Craig W. Lindsley

PII: S0960-894X(19)30781-4
DOI: https://doi.org/10.1016/j.bmcl.2019.126812
Reference: BMCL 126812

To appear in: *Bioorganic & Medicinal Chemistry Letters*

Received Date: 16 October 2019
Revised Date: 4 November 2019
Accepted Date: 6 November 2019

Please cite this article as: Temple, K.J., Engers, J.L., Long, M.F., Watson, K.J., Chang, S., Luscombe, V.B., Jenkins, M.T., Rodriguez, A.L., Niswender, C.M., Bridges, T.M., Jeffrey Conn, P., Engers, D.W., Lindsley, C.W., Discovery of a novel 2,3-dimethylimidazo[1,2-*a*]pyrazine-6-carboxamide M_4 positive allosteric modulator (PAM) chemotype, *Bioorganic & Medicinal Chemistry Letters* (2019), doi: https://doi.org/10.1016/j.bmcl.2019.126812

Graphical Abstract

To create your abstract, type over the instructions in the template box below.
Fonts or abstract dimensions should not be changed or altered.

Discovery of a novel 2,3-dimethylimidazo[1,2-*a*]pyrazine-6-carboxamide M_4 positive allosteric modulator (PAM) chemotype

Leave this area blank for abstract info.

Kayla J. Temple[a,b], Julie L. Engers[a,b], Madeline F. Long[a,b], Katherine J. Watson[a,b], Sichen Chang[a,b], Vincent B. Luscombe[a,b], Matthew T. Jenkins[a,b], Alice L. Rodriguez[a,b], Colleen M. Niswender[a,b,d], Thomas M. Bridges[a,b], P. Jeffrey Conn[a,b,d], Darren W. Engers[a,b*], Craig W. Lindsley[a,b,c*]

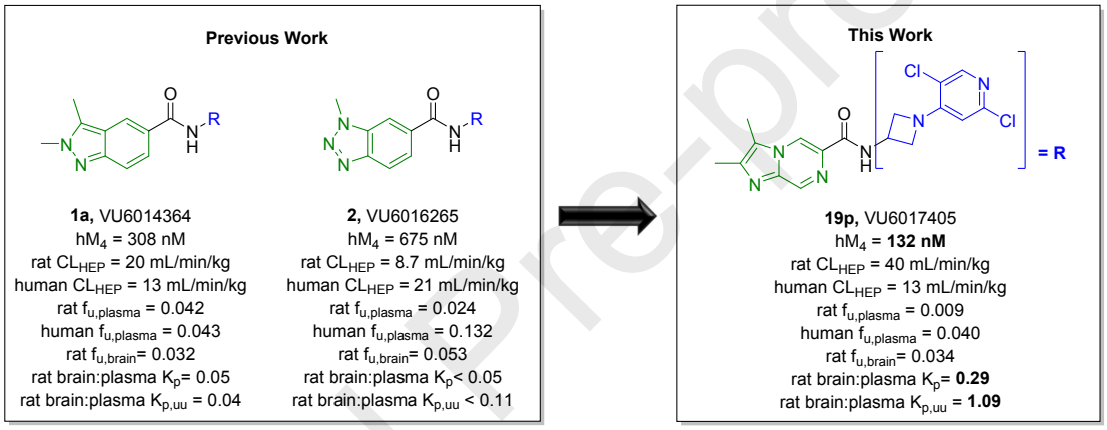

ELSEVIER

Bioorganic & Medicinal Chemistry Letters
journal homepage: www.elsevier.com

Discovery of a novel 2,3-dimethylimidazo[1,2-*a*]pyrazine-6-carboxamide M_4 positive allosteric modulator (PAM) chemotype

Kayla J. Temple[a,b], Julie L. Engers[a,b], Madeline F. Long[a,b], Katherine J. Watson[a,b], Sichen Chang[a,b], Vincent B. Luscombe[a,b], Matthew T. Jenkins[a,b], Alice L. Rodriguez[a,b], Colleen M. Niswender[a,b,d,e], Thomas M. Bridges[a,b], P. Jeffrey Conn[a,b,d,e], Darren W. Engers[a,b*], Craig W. Lindsley[a,b,c,e*]

[a]*Vanderbilt Center for Neuroscience Drug Discovery, Vanderbilt University, Nashville, TN 37232, USA*
[b]*Department of Pharmacology, Vanderbilt University School of Medicine, Nashville, TN 37232, USA*
[c]*Department of Chemistry, Vanderbilt University, Nashville, TN 37232, USA*
[d]*Vanderbilt Kennedy Center, Vanderbilt University School of Medicine, Nashville, TN 37232, USA*
[e]*Vanderbilt Institute of Chemical Biology, Vanderbilt University, Nashville, TN 37232, USA*

ARTICLE INFO

Article history:
Received
Revised
Accepted
Available online

Keywords:
M_4
Muscarinic acetylcholine receptor
Positive Allosteric modulator (PAM)
Structure Activity Relationship (SAR)

ABSTRACT

This Letter details our efforts to discover structurally unique M_4 PAMs containing 5,6-heteroaryl ring systems. In an attempt to improve the DMPK profiles of the 2,3-dimethyl-2H-indazole-5-carboxamide and 1-methyl-1*H*-benzo[*d*][1,2,3]triazole-6-carboxamide cores, we investigated a plethora of core replacements. This exercise identified a novel 2,3-dimethylimidazo[1,2-a]pyrazine-6-carboxamide core that provided improved M_4 PAM activity and CNS penetration.

Muscarinic acetylcholine receptor subtype 4 (M_4) positive allosteric modulators (PAMs) have garnered much attention as potential drug targets as novel treatments for various neurological disorders such as Parkinson's disease,[1] Huntington's disease,[2] and schizophrenia (both the positive and negative symptom clusters).[3-6] Recent efforts from our group have focused on eliminating the classical β-amino carboxamide pharmacophore of many historical M_4 PAMs as this moiety engenders physiochemical and DMPK properties that preclude candidate development.[7-15] While our endeavors to date have provided structurally distinct potent human and rat M_4 PAMs, the DMPK profiles of said compounds have been rather lackluster. Previously, we reported several new M_4 PAM chemotypes, two of which are depicted in **Figure 1**, analogs **1a & 2**.[16] These analogs exemplify new M_4 PAM chemotypes that possess activity, yet leave much to be desired in terms of pharmacological profiles.

In a new venture to identify novel M_4 PAM chemotypes possessing improved DMPK profiles, we elected to pursue a scaffold hopping approach utilizing teh structures of 1a and 2 as a starting point. In this Letter, we will discuss the scaffold hopping exercise and the identification of fundamentally new M_4 PAM chemotypes. In general, we wished to explore a large selection 5,6-heteroaryl ring systems lacking the β-amino carboxamide moiety.

Our study began with modifications to the 3-methyl-1H-indazole core of **1a (Table 1)**. First, we optimized our original methylation protocol, which gave predominately the undesired

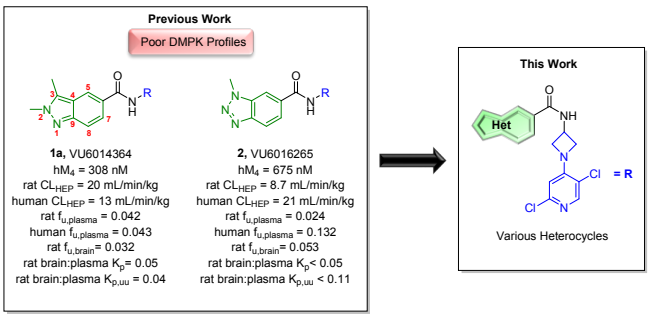

Figure1. Scaffold hopping concept from M_4 PAMs **1a** and **2** to generate structurally unique M_4 PAM chemotypes.

1,3-dimethylated indazole (**Scheme 1**). Instead, we chose to use the methyl Meerwein salt, which provided the desired 2,3-dimethylated indazole as the major product. With our optimal conditions in hand, various commercial 5-bromo-3-substituted-

1H- and either trimethyloxonium tetrafluoroborate or triethyloxonium tetrafluoroborate (**1d-h**). To generate fluorinated analogs **1b** and **1c**, we first needed to synthesize indazoles **11** and **15 (Scheme 2)**. Analog **11** could readily be synthesized by condensing hydrazine with commercially available 2'-fluoroacetophenone **9** to yield intermediate **10** which was then methylated to afford bromide **11**.

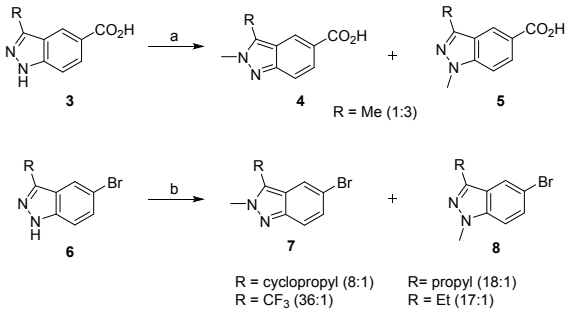

Scheme 1. Methylation conditions of 3-substituted indazoles. Reagents and conditions: (a) MeI, K_2CO_3, DMF, rt; (b) Me_3OBF_4, EtOAc, rt.

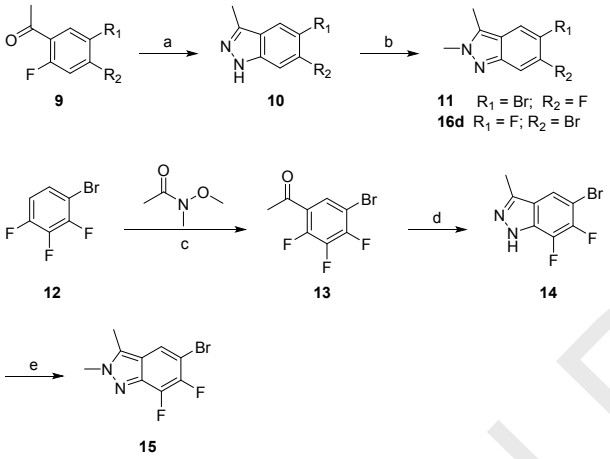

Scheme 2. Synthesis of non-commercial fluorinated indazoles **11**, **15**, & **16d**. Reagents and conditions: (a) NH_2NH_2, 1-butanol, µW 180 °C, 1h; (b) Me_3OBF_4, EtOAc, rt, 5h, 52-55% (over 2 steps); (c) LDA, THF, -78 °C, 1h, then rt, 18h, 55%; (d) NH_2NH_2, 1-butanol, µW 180 °C, 1h; (e) Me_3OBF_4, EtOAc, rt, 60% (over 2 steps).

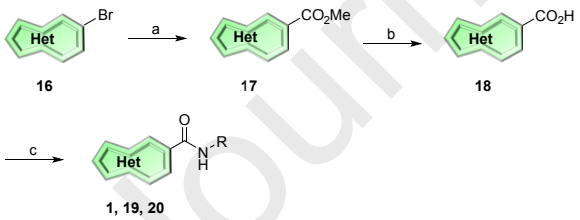

Scheme 3. Synthesis of M_4 PAM analogs **1, 19,** and **20**. Reagents and conditions: (a) $Pd(dppf)Cl_2$, Et_3N, MeOH/DMF (1:1), CO, 80 °C, 18 h; (b) NaOH, MeOH/H_2O (5:1); (c) RNH_2, HATU, DIEA, DMF.

The synthesis of **15** began with treating 1-bromo-2,3,4-trifluorobenzene, **12**, with LDA followed by N-methoxy-N-methylacetamide to afford the acetylated intermediate **13**. This 2'-fluoroacetophenone intermediate was condensed with hydrazine followed by methylation with the Meerwein salt to give bromide **15**. With the 5-bromoindazole intermediates in hand (**16**), we utilized common Pd-catalyzed carbonylation conditions to generate the methyl esters **17 (Scheme 3)**. Following saponification of the methyl ester to the carboxylic acid, intermediates **18** underwent HATU coupling with 1-(2,5-dichloropyridin-4-yl)azetidin-3-amine to afford analogs **1a-h**. All ELSD). After evaluating analogs **1** against human M_4, it became very clear that minor modifications to the 2,3-dimethylated indazole core lead to a decrease in potency (**Table 1**).

This initial exercise led us to turn our attention to evaluating new 5,6-heteroaryl ring systems as potential M_4 PAM cores. The bromide or carboxylic acid precursors (**16** or **18**) for several of these cores were commercially available (**19e**, **19g**, **19i**, and **19l**)

Table 1. Structures and activities for analog **1**.

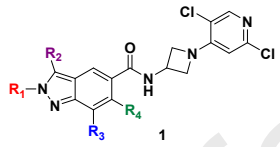

Cpd	R_1	R_2	R_3	R_4	hM4 EC_{50} (nM) [a] [% ACh Max]
a	CH_3	CH_3	H	H	308 [64]
b	CH_3	CH_3	H	F	739 [68]
c	CH_3	CH_3	F	F	2540 [54]
d	Et	CH_3	H	H	Inactive
e	CH_3	Et	H	H	584 [34]
f	CH_3	CF_3	H	H	Inactive
g	CH_3	CF_2	H	H	Inactive
h	CH_3		H	H	Inactive

[a] Calcium mobilization assays with $hM_{4/Gqi5}$-CHO cells performed in the presence of an EC_{20} fixed concentration of acetylcholine, n =1 experiments performed in triplicate.

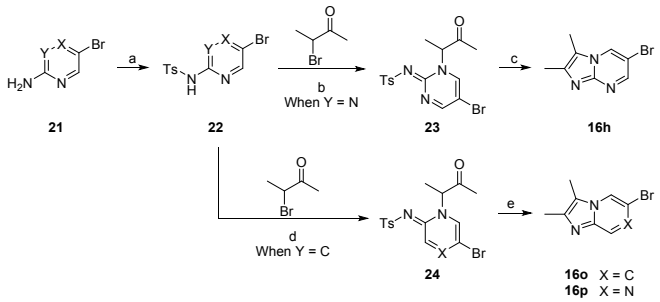

Scheme 4. Synthesis of M_4 PAM intermediate **16h**, **16o**, and **16p**. Reagents and conditions: (a) pTsCl, pyridine, 90 °C, 18h, 64-94%; (b) i. DIEA, DMF, 0 °C, 30 min; ii. 3-bromo-2-butanone, rt, 18h, 81%; (c) TFAA, THF, 0 °C then 60 °C, 3h, 71%; (d) i. NaH, DMF, 0 °C then rt, 30 min; ii. 3-bromo-2-butanone, rt, 18h, 60 - 94 %; (c) TFAA, THF, 0 °C then 60 °C, 3h, 80 - 87%.

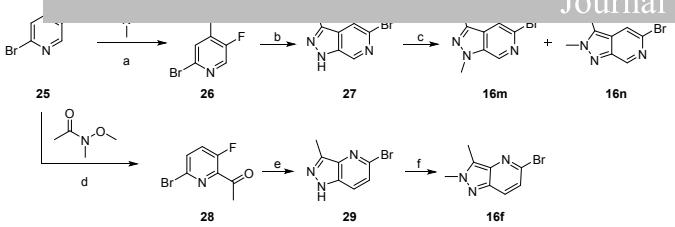

Scheme 5. Synthesis of M_4 PAM intermediates **16f**, **16m** and **16n**. Reagents and conditions: (a) i. LDA, THF, -78 °C, 4h; ii. *N*-methoxy-*N*-methylacetamide, THF, -78 °C to rt, 18h, 60%; (b) NH_2NH_2, 1-butanol, µW 180 °C, 2h; (c) K_2CO_3, MeI, DMF, rt, 3h, 31% (**16m** – over 2 steps) and 19% (**16n** – over 2 steps); (d) i. *n*-BuLi, Et_2O, -78 °C, 2h; ii. N-methoxy-N-methylacetamide, Et_2O, -78 °C, 1.5h, 51%; (e) NH_2NH_2, 1-butanol, µW 180 °C, 2h; (f) K_2CO_3, MeI, DMF, rt, 18h, 19%.

Table 2. Structure and activities for analog **19**.

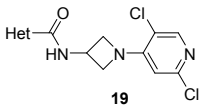

19

Cpd	Het	hM4 EC_{50} (nM) [a] [% ACh Max]
a	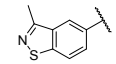	Inactive
b	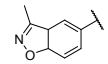	Inactive
c	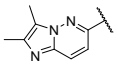	Inactive
d	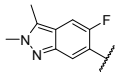	Inactive
e	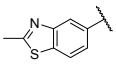	494 [37]
f	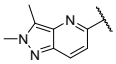	Inactive
g	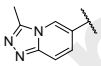	>10000 [52]
h	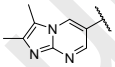	849 [99]
i		746 [62]
j	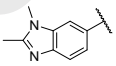	654 [73]
k	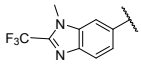	468 [53]
l	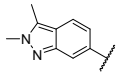	420 [35]
m		375 [68]
n	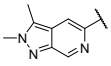	370 [86]
o	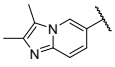	243
p	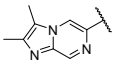	132 [89]

[a] Calcium mobilization assays with $hM_{4/Gqi5}$-CHO cells performed in the presence of an EC_{20} fixed concentration of acetylcholine, n =1 experiment performed in triplicate.

while others were synthesized according to established protocols (**19a**, **19b**, **19c**, **19j**, and **19k**).[17-20] Intermediate 6-bromo- 2,3-dimethylimidazo[1,2-a]pyrimidine (**16h**) was synthesized by first tosylating 5-bromopyrimidin-2-amine (**21**) followed by alkylation with 3-bromo-2-butanone utilizing DIEA as the base afforded intermediate **23**, which readily cyclized to **16h** in the presence of trifluoroacetic anhydride **(Scheme 4)**. Intermediates **16o** and **16p** were constructed in a similar manner; however, we found it was

Table 3. Structure and activities for analog **20**.

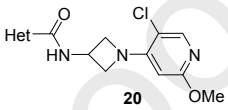

20

Cpd	Het	hM4 EC_{50} (nM) [a] [% ACh Max]
a	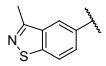	Inactive
b		Inactive
c	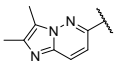	Inactive
d	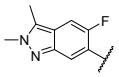	Inactive
e	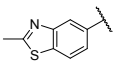	Inactive
f	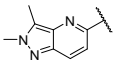	Inactive
g	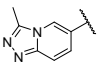	>10000 [31]
h	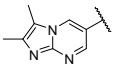	1832 [95]
i		Inactive
j	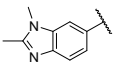	1384 [51]
k	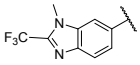	940 [38]
l	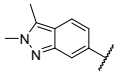	3882 [35]
m	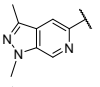	1422 [55]
n	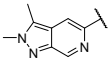	454 [57]
o	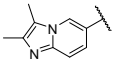	1153
	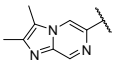	

p	430	[83]

[a] Calcium mobilization assays with $hM_{4/Gqi5}$-CHO cells performed in the presence of an EC_{20} fixed concentration of acetylcholine, n =1 experiment performed in triplicate.

crucial that sodium hydride be substituted for DIEA to obtain high yields. Pyrazolo[3,4-c]pyridines **16m** and **16n** were synthesized from 2-bromo-5-fluoropyridine (**25**), which could be selectively acetylated *para* to the pyridine nitrogen when LDA was employed as a base to afford the 2'-fluoroacetophenone **26 (Scheme 5)**. Alternatively, to synthesize **16f**, 2-bromo-5- fluoropyridine could be selectively acetylated *ortho* to the pyridine nitrogen when *n*-BuLi was substituted as the base to give the 2'-fluoroacetophenone **28**. Both intermediates **26** and **28** were condensed with hydrazine followed by methylation with potassium carbonate and methyl iodide. It should be noted that we did not utilize the methyl Meerwein salt in this instance as it predominately yielded the trimethyl tertiary amine salt. With the commercial and in-house generated intermediates in hand, final analogs **19** and **20** were readily synthesized according to **Scheme 3**. Amino azetidines of **19** and **20** were chosen for this exercise based on past studies.

Select analogs **19** and **20** were screened against human M_4 (hM_4) to determine potency, with results highlighted in **Tables 2 & 3**. This exercise resulted in several analogs that possess M_4 PAM functional potencies less than 500 nM in both human and rat: **19k** (hEC_{50} = 468 nM; rEC_{50} = 378 nM), **19n** (hEC_{50} = 370 nM; rEC_{50} = 331 nM), **19o** (hEC_{50} = 243 nM; rEC_{50} = 433 nM), **19p** (hEC_{50} = 132 nM; rEC_{50} = 233 nM), **20n** (hEC_{50} = 454 nM; rEC_{50} = 339 nM), and **20p** (hEC_{50} = 430 nM; rEC_{50} = 295 nM). Interestingly, changing the 2-chloro substituent of 1-(2,5-dichloropyridin-4-yl)azetidin-3-amine to a methoxy substituent typically led to a 2-9 fold decrease in potency with one analog ranked as inactive (**19i** vs. **20i**). In previous series, these two amines often gave similar potency profiles.

Benzothiazoles, benzoisothiazoles and benzoisoxaoles were generally not tolerated (**19a**, **19b**, **19e**, **202a**, **20b**, **20e**). It was also noted that placement of an additional nitrogen within the 5,6-ring systems was crucial for activity or lack thereof. For example, modification of the original 2,3-dimethyl-2*H*-indazole core of **1a** the 5,6-ring **(Figure 1)** to yield 2,3-dimethyl-2H-pyrazolo[4,3-b]pyridine **19f** led to a complete loss of activity. Alternatively, addition of a nitrogen at the 7-position afforded 2,3-dimethyl-2H-pyrazolo[3,4-c]pyridine **19n** (hM_4 EC_{50} = 370 nM), which displayed comparable potency to **1a**.

These trends were also observed with the most potent core of the series: 2,3-dimethylimidazo[1,2-a]pyridine **19o** (hM_4 EC_{50} = 243 nM). In comparison, when inserting a nitrogen at the 5-position of the ring system to afford 2,3-dimethylimidazo[1,2-b]pyridazine **19c**, a complete loss of activity was observed. Likewise, addition of a nitrogen at the 2-position to give 3-methyl-[1,2,4]triazolo[4,3-a]pyridine **19g** led to a >40-fold loss in potency; however, addition of a nitrogen at the 8-position to yield 2,3-dimethylimidazo[1,2-a]pyrimidine **19h** led to only a ~3.5-fold loss in potency. On the other hand, addition of a nitrogen at the 7-position gave 2,3-dimethylimidazo[1,2-*a*]

Table 3. *In vitro* DMPK and rat PBL data for select analogs **19** and **20**.

Property	19m VU6016371	19n VU6016376	20n VU6016377	19o VU6017410	19p VU6017405	20p VU6017406
MW	391.25	391.25	386.84	390.27	391.25	386.84
xLogP	1.71	1.17	1.06	3.08	1.69	1.03
TPSA	75.9	75.9	85.2	62.5	75.4	84.7
In vitro PK parameters						
CL_{INT} (mL/min/kg), rat	85	59	33	130	96	83
CL_{HEP} (mL/min/kg), rat	38	32	23	46	40	38
CL_{INT} (mL/min/kg), human	28	26	28	39	33	25
CL_{HEP} (mL/min/kg), human	12	12	12	14	13	11
Rat fu_{plasma}	0.011	0.022	0.022	0.013	0.009	0.017
Human fu_{plasma}	0.039	0.014	0.017	0.030	0.040	0.045
Rat fu_{brain}	0.021	0.030	0.032	0.027	0.034	0.021
$K_{p,\ brain:plasma}$	<0.24	0.30	0.67	0.10	0.29	<1.08
$K_{puu,\ brain:plasma}$	<0.45	0.41	0.97	0.21	1.09	<1.33

19p (hM_4 EC_{50} = 132 nM) which was 2-fold more potent than **19o**.

Of these compounds, **19m**, **19n**, **20n**, **19o**, **19p**, and **20p** were advanced into a battery of *in vitro* DMPK assays (**Table 4**) and our standard rat plasma:brain level (PBL) IV cassette paradigm. In regard to physicochemical properties, all six analogs possess molecular weights less than 400 Da, with two having attractive CNS xLogPs (3.11 and 3.08). The new 5,6-ring systems evaluated displayed moderate predicted hepatic clearance based on microsomal CL_{int} in both human (CL_{hep}s of 12 – 14 mL/min/kg) and rat (CL_{hep}s of 23 - 46 mL/min/kg). When compared to cores **1a** and **2 (Figure 1)**, the human clearance values of our new scaffolds were comparable; however, rat clearance values were slightly higher.

All compounds evaluated (rat f_us 0.009 – 0.022; rat f_us brain 0.021 – 0.034; human f_us 0.014 – 0.045) were more bound to plasma proteins when compared to **1a** or **2.** While **1a** and **2** proved to have limited CNS penetration (rat brain:plasma $K_p \leq 0.05$, $K_{p,uu} < 0.11$), all six novel 5,6-ring systems examined showed improved CNS penetration with **19p** (K_p = 0.29, $K_{p,uu}$ = 1.09), **20p** (K_p <1.08, $K_{p,uu}$ < 1.33), and **20n** (K_p = 0.67, $K_{p,uu}$ = 0.97) being superior. Interestingly, these analogs incorporated a nitrogen at the 7-position of the 5,6-ring system.

In summary, a scaffold hopping exercise based on M_4 PAMs **1a** and **2** identified two novel cores: a 2,3-dimethyl-2H-pyrazolo[3,4-c]pyridine-5-carboxamide core (**19n** & **20n**) and a 2,3-dimethylimidazo[1,2-a]pyrazine-6-carboxamide core (**19p**).

Ana... ...hotic activity when compared to **1a** or **2**, respectively. While this analog displayed a 2-fold increase in rat CL_{hep} and was more bound to rat plasma proteins than **1a**, all other protein binding values were similar. Moreover, **19p** possessed improved brain:plasma K_p and $K_{p,uu}$ values in relation to **1a**. Although this endeavor did not deliver M_4 PAMs with the desired DMPK profiles to advance as potential development candidates, it did garner insights to further our goals, which will be disclosed in due course.

Acknowledgments

We thank the NIH for funding via the NIH Roadmap Initiative 1x01 MH077607 (C.M.N.), the Molecular Libraries Probe Center Network (U54MH084659 to C.W.L.) and U01MH087965 (Vanderbilt NCDDG). We also thank William K. Warren, Jr. and the William K. Warren Foundation who funded the William K. Warren, Jr. Chain in Medicine (to C.W.L.).

References and notes

1. Shen W, Plotkin JL, Francardo V, et al. M_4 Muscarinic receptor signaling ameliorates striatal plasticity deficits in models of L-DOPA-induced dyskinesia. *Neuron*. 2015;88:762-773.
2. Pancani T, Foster DJ, Moehle MS, et al. Allosteric activation of M_4 muscarinic receptors improve behavioral and physiological alteration in early symptomatic YAC128 mice. *Proc Natl Acad Sci USA*. 2015;112:14078-14083.
3. Bridges TM, LeBois EP, Hopkins CR, et al. The antipsychotic potential of muscarinic allosteric modulation. *Drug News Perspect.* 2010;23:229-240.
4. Foster DJ, Wilson JM, Wess J, et al. Antipsychotic-like effects of M_4 positive allosteric modulators are mediated by CB2 receptor-dependent inhibition of dopamine release. *Neuron.* 2016;91:1244-1252.
5. Jones CK, Byun N, Bubser M. Muscarinic and nicotinic acetylcholine receptor agonists and allosteric modulators for the treatment of schizophrenia. *Neuropsychopharmacology.* 2012;37:16-42.
6. Farrell M, Roth BL. Allosteric antipsychotics: M_4 muscarinic potentiators as novel treatments for schizophrenia. *Neuropsychopharmacology*. 2010;35:851-852.
7. Chan WY, McKinzie DL, Bose S, et al. Allosteric modulation of the muscarinic M_4 receptor as an approach to treating schizophrenia. *Proc Natl Acad Sci USA*. 2008;105:10978-10983.
8. Leach K, Loiacono RE, Felder CC, et al. Molecular mechanisms of action and *in vivo* validation of an M_4 muscarinic acetylcholine ... properties. *Neuropsychopharmacology*. 201;33:853-869.
9. Brady A, Jones CK, Bridges TM, et al. Centrally active allosteric potentiators of the M_4 muscarinic acetylcholine receptor reverse amphetamine-induced hyperlocomotor activity in rats. *J Pharm Exp Ther*. 2008;327;941-953.
10. Byun NE, Grannan M, Bubser M, et al. Antipsychotic drug-like effects of the selective M_4 muscarinic acetylcholine receptor positive allosteric modulator VU0152100. *Neuropsychopharmacology*. 2014;39:1578-1593.
11. Bubser M, Bridges TM, Dencker D, et al. Selective activation of M_4 muscarinic acetylcholine receptors reverses MK-801-induced behavioral impairments and enhances associative learning in rodents. *ACS Chem Neurosci.* 2014;5:920-942.
12. Melancon BJ, Wood MR, Noetzel MJ, et al. Optimization of M_4 positive allosteric modulators (PAMs): The discovery of BU0476406, a non-human primate *in* vivo tool compound for translational pharmacology. *Bioorg Med Chem Lett.* 2017;27:2296-2301.
13. Wood MR, Noetzel J, Melancon BH, et al. Discovery of VU0467485/AZ13713945: An M_4 PAM evaluated as a preclinical candidate for the treatment of Schizophrenia. *ACS Med Chem Lett.* 2017;8:233-238.
14. Long MF, Engers JL, Chang S, et al. Discovery of a novel 2,4-dimethylquinolin-6-carboxamide M_4 positive allosteric modulator (PAM) chemotype via scaffold hopping. *Bioorg Med Chem Lett.* 2017;27:4999-5001.
15. Temple KJ, Engers JL, Long MF, et al. Discovery of a novel 3,4-dimethylcinnoline carboxamide M4 positive allosteric mosulator (PAM) chemotype via scaffold hopping. *Bioorg Med Chem Lett.* 2019, 19, article 126678.
16. Temple KJ, Long MF, Engers JL, et al. Development of structurally distinct tricyclic M_4 positive allosteric modulator (PAM). *Bioorg Med Chem Lett.* Manuscript submitted.
17. Fink DM, Strupczewski JT. Preparation of 6-fluorobenziothiazoles via a regioselective nucleophilic aromatic substitution reaction. *Tetrahedron Lett*. 199;34:6525-6528.
18. Pollak A, Stanovnki B, Tišler M. Synthesis of pyridazine derivatives – XVI: Methyl substituted imadazo(1,2-b)pyridazines by synthesis and hemolytic methylation. *Tetrahedron.* 1968;24:2623-2629.
19. Soria-Arteche O, Hernández-Campos A, Yépez-Mulia L, et al. Synthesis and antiprotozoal activity of nitazoxanide-*N*-methylbenzimidazole hybrids. *Bioorg Med Chem Lett.* 2013;23:6838-3841.
20. Zhang M, Zhang Y, Song M, et al. Structure-based discovery and optimization of benzo[d]isoxaole derivatives as potent and selective BET inhibitors for potential treatment of castration-resistant prostate cancer (CRPC). *J Med Chem*. 2018;6:3037-3058.

Highlights

- Discovery of two novel tricyclic-based M_4 PAMs
- Utility of scaffold hopping to improve potency/properties/DMPK
- Balanced human and rat M_4 PAM potency
- Rare 8,9-dimethyl-8*H*-pyrazolo[3,4-*h*]quinazoline and 1-methyl-1*H*-[1,2,3]triazolo[4,5-*h*]quinazoline cores